

## Lipopeptides

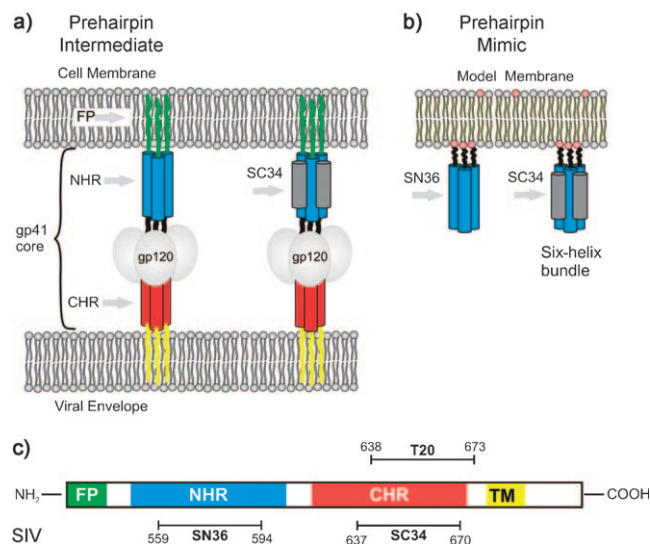
## Coiled-Coil Lipopeptides Mimicking the Prehairpin Intermediate of Glycoprotein gp41

Steffen Schuy, Edith Schäfer, Nicholas C. Yoder, Stephan Hobe, Krishna Kumar, Reiner Vogel, and Andreas Janshoff\*

A decisive molecular step in retroviral fusion has been modeled by rational design of lipopeptide assemblies that mimic a coiled-coil structure serving as a receptor for potential antagonists. Binding of antagonists to surface-confined coiled-coil structures has been quantified by ellipsometry and visualized by atomic force microscopy (AFM). The envelope (ENV) glycoproteins of human and simian immunodeficiency viruses (HIV and SIV) play an essential role in the early stage of virus entry.<sup>[1]</sup> ENV consists of two protein domains called gp120 and gp41. The surface subunit gp120 binds to receptors and coreceptors of the host cell, while the gp41 subunit mediates fusion of the virus with the host-cell membrane.<sup>[2,3]</sup>

Binding of gp120 results in a major conformational change, in which gp41 is exposed and adopts a prehairpin intermediate (PI) conformation. The PI (Scheme 1 a) consists of a trimeric central coiled coil created by the N-terminal heptad repeat (NHR) unit displaying three conserved hydrophobic grooves that serve as binding sites for the corresponding C peptides from the C-terminal heptad repeat (CHR) region. The next step, which is believed to be crucial for overcoming the activation barrier for fusion of the host-cell membrane with the viral envelope, involves the antiparallel packing of the CHR region against this central coiled coil, thus forming a six-helix bundle, referred to as the trimer-of-hairpin conformation.<sup>[3–5]</sup> Interference with this rate-limiting step is an effective way to abolish viral infection at an early stage.<sup>[1,2,6–10]</sup>

The inevitable complexity of the native fusion machinery requires a rational design of the crucial conformational switch from the prehairpin intermediate to the trimer of hairpins in order to establish an efficient sensor platform for antagonist screening. Scheme 1 b illustrates our approach, in which the prehairpin intermediate of SIV serves as a recognition site for



**Scheme 1.** Native prehairpin intermediate (a) and the corresponding mimic (b). c) Sequence of gp41 from SIV (FP = fusion peptide, NHR = N-terminal heptad repeat unit, CHR = C-terminal heptad repeat unit, TM = transmembrane subunit). The residue numbers correspond to their positions in gp160 of SIV (strain Mac239).

potential inhibitors derived from the corresponding C peptides from the CHR region, such as SC34. Binding of SC34 precludes the formation of the trimer-of-hairpins structure, which is essential for successful virus fusion.

The assay is based on covalently attached lipid anchors (1,2-dioleoyl-*sn*-glycero-3-phosphoethanolamine-*N*-[4-(*p*-maleimidomethyl)cyclohexanecarboxamide], MCC-DOPE), which were employed instead of fusion peptides (FP) to drive the N peptides of SIV (SN36) into the desired coiled-coil conformation on a solid-supported model membrane. Binding of antagonists to this prehairpin mimic is thought to model the natural formation of a trimer-of-hairpins conformation. Strong binding should therefore prevent the decisive fusion step by forming a stable analogue.<sup>[11]</sup> Coupling of SN36 extended with an N-terminal cysteine moiety (CGG) was carried out on a preformed solid-supported membrane doped with 10 mol % MCC-DOPE (see the Experimental Section).

Formation of the MCC-DOPE-SN36 conjugate was monitored by means of circular dichroism (CD), FTIR spectroscopy, ellipsometry, and atomic force microscopy (AFM; see Figure 1 and the Supporting Information). CD spectra (Figure 1 a) of SN36 in solution clearly show that the peptide adopts a predominately random-coil conformation,<sup>[11]</sup> while covalent coupling to MCC-DOPE-containing DOPC liposomes results in a prevailing  $\alpha$ -helical structure (DOPC =

[\*] S. Schuy, E. Schäfer, Prof. Dr. A. Janshoff  
Institute of Physical Chemistry  
University of Göttingen, 37077 Göttingen (Germany)  
E-mail: ajansho@gwdg.de

Dr. S. Hobe  
Institute of General Botany (Plant Physiology)  
University of Mainz, 55128 Mainz (Germany)

Dr. N. C. Yoder, Prof. Dr. K. Kumar  
Department of Chemistry  
Tufts University, Medford MA 02155 (USA)

Dr. R. Vogel  
Institute for Molecular Medicine and Cell Research  
University of Freiburg, 79104 Freiburg (Germany)

Supporting information for this article is available on the WWW under <http://dx.doi.org/10.1002/anie.200803080>.

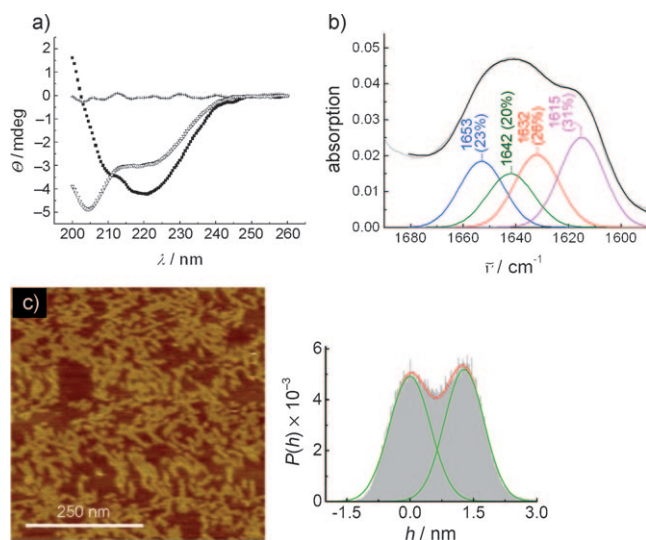


**Figure 1.** a) CD spectra of DOPC liposomes functionalized with 10 mol% MCC-DOPE-SN36 (■), SN36 peptides dissolved in phosphate-buffered saline (PBS; ▽), and DOPC vesicles (+) that were incubated with SN36 and subsequently gel-filtrated. b) FTIR spectra of SN36 attached to fully hydrated DOPC/MCC-DOPE-SN36 (9:1) multilamellar bilayer stacks in  $\text{D}_2\text{O}$ . The gray trace is the experimental spectrum; the black trace is the sum of the bands found by deconvolution. c) AFM image and normalized height histogram  $P(h)$  of a DOPC/MCC-DOPE-SN36 (9:1) bilayer after rinsing with buffer;  $h=0$  corresponds to the bilayer surface.

1,2-dioleoyl-*sn*-glycero-3-phosphocholine). Nonspecific interaction of SN36 with pure DOPC vesicles was not observed. We consider the formation of  $\alpha$  helices as a first indication that coiled-coil complexes may have been formed as a result of proximal confinement on the bilayer.

Coiled coil formation was further investigated by FTIR spectroscopy of the amide I band of fully deuterated MCC-DOPE-SN36 in hydrated multilamellar bilayer stacks (see Figure 1b and the Supporting Information). The spectral maxima of the amide I region are located well below the classical  $\alpha$ -helical band ( $1651\text{ cm}^{-1}$ ), that is, at  $1643\text{ cm}^{-1}$ , indicative of coiled-coil aggregates.<sup>[12–14]</sup> Peak deconvolution of the amide I band revealed a distinctive four-band pattern with maxima at 1615, 1632, 1642, and  $1653\text{ cm}^{-1}$ . Bands at very low wavenumbers in the amide I region are often found in spectra of aggregated proteins and have been attributed to intermolecular contacts of extended-chain segments. The changes attributed to such aggregation include broadening and a shift to low wavenumbers, which is accompanied by the emergence of a well-defined component band at  $1616\text{ cm}^{-1}$ .<sup>[15]</sup> For comparison, Heimburg and Marsh report band positions of 1615, 1631, 1641, and  $1651\text{ cm}^{-1}$  for the amide I band of GCN4-p11I, which is known to form coiled coils.<sup>[12]</sup> As demonstrated in the literature, there is an inverse correlation between the pitch length of a coiled coil (in this case  $175\text{ \AA}$ ) and the spectral maximum of the amide I region.<sup>[11,14]</sup> Assuming that the pitch length is not altered by peptide coupling to the lipid anchor, the spectral maximum of MCC-DOPE-SN36 ( $1643\text{ cm}^{-1}$ ) correlates well with the spectral maximum of GCN4-p11I zippers ( $1644\text{ cm}^{-1}$ ), which also exhibit a pitch length of  $175\text{ \AA}$  and are known to assemble

into trimeric coiled coils.<sup>[16]</sup> Taken together, CD and FTIR spectroscopy strongly support formation of coiled-coil structures anchored to the bilayer.

The topological structure of MCC-DOPE-SN36 assemblies within a phospholipid bilayer was visualized by in situ AFM. Figure 1c shows a tapping mode AFM image of SN36 coupled in situ to maleimide-functionalized solid-supported DOPC/MCC-DOPE (9:1; DOPC\*) bilayers. After coupling, the previously flat bilayer surface displays the small lateral aggregates with a uniform height of  $(2 \pm 0.3)\text{ nm}$  and lateral dimensions (width  $\times$  length) of roughly  $2 \times 20\text{ nm}^2$  on top of its surface.

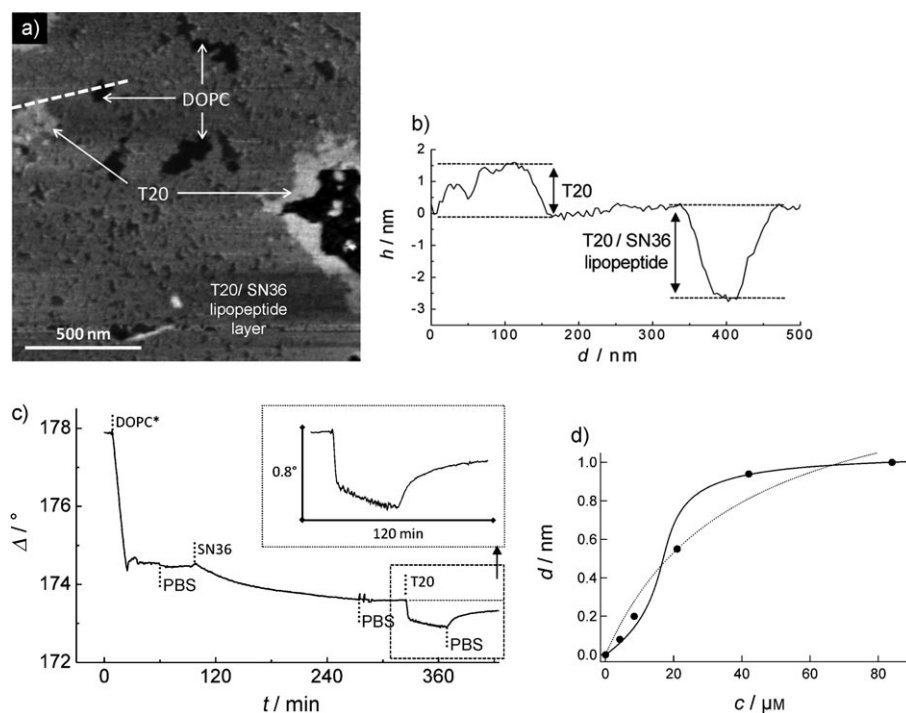
We then investigated inhibitor binding to the coiled-coil assembly on the membrane surface. For this purpose, we carried out AFM imaging and time-resolved ellipsometry to monitor topographic changes in conjunction with binding kinetics. Two inhibitor sequences were used, T20 (also known as fuzeon) and SC34 originating from gp41 of SIV (Scheme 1c).

Figure 2a shows an AFM image after addition of T20 to a DOPC/MCC-DOPE-SN36 (9:1) bilayer on mica. The image clearly reveals that the ribbon-like structure of the SN36 assemblies has been changed. Instead, a homogeneous coverage of peptide aggregates exhibiting an average height of  $(2 \pm 0.2)\text{ nm}$  over the bilayer surface has formed. The elevation is essentially identical to the height of the neat SN36 lipopeptide assemblies ( $2\text{ nm}$ ), giving rise to an overall thickness of  $5.7\text{--}6\text{ nm}$ . Frequently, an additional step of  $1.5\text{ nm}$  on top of the SN36-T20 structures could be detected (Figure 2b and the Supporting Information).

The substantial increase in surface coverage is attributed to adjacent binding of peptides to the preformed clusters of MCC-DOPE-SN36 causing lateral expansion of the first peptide monolayer. It is known that the mode of interaction of T20 with N36 peptides is more variable than that of the SC34 peptide and might lead to complexes other than a six-helix bundle, which might also explain the occasional height increase.<sup>[4,17]</sup> After heating the sample to  $65^\circ\text{C}$  for 20 min and rinsing with buffer at  $65^\circ\text{C}$ , the characteristic ribbon structure of the SN36 assemblies emerges again and the additional peptide domains, which resulted from addition of T20, disappear (see the Supporting Information). Hence, we conclude that heating efficiently breaks the noncovalent complex, as expected from solution studies.<sup>[11]</sup> It was possible to repeat these steps several times without losing the binding ability of the SN36 coiled-coil receptors.

These findings are corroborated by time-resolved ellipsometric data (Figure 2c) of the full process starting from pure silicon exposed to DOPC\* vesicles followed by SN36 coupling and addition of T20 or SC34.

The experiment starts with the formation of a MCC-DOPE-functionalized DOPC bilayer (DOPC\*) on a silicon surface exhibiting a thickness of  $d = (3.7 \pm 0.2)\text{ nm}$ .<sup>[18]</sup> Between steps, the solution was exchanged with fresh PBS. Subsequent addition of  $100\text{ nmol}$  SN36 resulted in a significant decrease of the  $\Delta$  values over time, resulting in a final layer thickness of  $d_{\text{SN36}} = (1.3 \pm 0.3)\text{ nm}$ , assuming a continuous peptide layer with a refractive index of  $n_{\text{pep}} = 1.50$ . Addition of SC34 (see the Supporting Information) or T20



**Figure 2.** a) AFM image of a DOPC/MCC-DOPE-SN36 (9:1) bilayer after addition of 25 nmol T20. b) Height analysis along the white dashed line in (a). c) Time course of the  $\Delta$  values obtained from ellipsometric measurements during the bilayer formation and in situ coupling reaction of SN36 to a DOPC/MCC-DOPE (9:1) bilayer and subsequent exposure to 25 nmol T20. d) Adsorption isotherm of T20 binding to MCC-DOPE-SN36 showing the apparent thickness  $d$  as a function of T20 concentration  $c$ . The dashed line corresponds to a Langmuir isotherm with a maximal shift in thickness of  $d_m = 1.56$  nm and a binding constant of  $K_L = 0.026 \mu\text{M}^{-1}$ . The solid line represents the Bragg-Williams isotherm assuming a moderate cooperativity of 1.55 and a binding constant of  $0.058 \mu\text{M}^{-1}$  (see the Supporting Information).

led to an additional decrease in  $\Delta$  values. Note that we cannot distinguish an increase in coverage of the first peptide monolayer from a second submonolayer on top of the first one. Subsequent rinsing with buffer after adsorption of T20 or SC34 resulted in partial desorption of the inhibitor peptide (Figure 2c). Figure 2d shows the corresponding adsorption isotherm of T20 binding to a SN36 functionalized DOPC\* bilayer. The dotted line denotes a Langmuir isotherm fitted to the data, while the solid line corresponds to regression with a Bragg-Williams isotherm reflecting the sigmoidal shape of the experimental isotherm, which is indicative of cooperative binding (see the Supporting Information). We found a binding constant of  $K_{BW} = 0.058 \mu\text{M}^{-1}$  that corresponds to half-maximal binding at  $17 \mu\text{M}$  for T20/SN36. Liu et al. report an  $IC_{50}$  of  $4.6 \mu\text{M}$  for T20 coupling to N46 using isothermal titration calorimetry.<sup>[22]</sup> N46 represents the full NHR sequence, which might be important for achieving higher affinities. Notably, inhibition of viral fusion (HIV) in cell–cell assays is reached at substantially lower T20 concentrations (ca. 20 nM), which might be attributed to a different mechanism of interaction between T20 and gp41.<sup>[22]</sup> Cooperative adsorption can be envisioned by the particular binding mechanism of C peptides to the NHR region. Receptor affinity of the trimeric SN36 bundles might increase with the number of T20 units attached to the PI conformation.

Control experiments using neat DOPC bilayers did not show any inhibitor adsorption on solid-supported membranes (see the Supporting Information), and thus we conclude that T20 and SC34 bind specifically and partly reversibly to the prehairpin mimic.

CD spectroscopy of the SC34/MCC-DOPE-SN36 complex formed on liposomes shows an increase in  $\alpha$  helicity, providing additional support that in fact native-like aggregates resembling the six-helix bundles composed of C peptides and membrane-anchored coiled-coil structures were formed (see the Supporting Information).

In conclusion, we could introduce the first membrane-based in vitro assay for viral fusion inhibitor detection employing a prehairpin mimic based on artificial lipopeptides.

## Experimental Section

**Materials:** Lipids were purchased from Avanti Polar Lipids (Alabaster, AL, USA) and chemicals for peptide synthesis were from Novabiochem (Darmstadt, Germany). T20 (fuzeon, T20: YTSLIHSLIEESQNQQEKNEQELL-ELDKWASLWNWF) was a gift from Roche Pharma (Mannheim, Germany).

**Peptide synthesis:** CGG-SN36 (Ac-CGGAGIVQQQQLLD-VVKRQQELLRLTVWGTKNLQTRVT) and SC34 (Ac-WQEWKRVDFLEENITALLEEAIQOEKNMYELQ) were synthesized using *tert*-butoxycarbonyl (tBoc) chemistry according to Schnölzer et al.<sup>[19]</sup> Crude acetylated peptides were purified by RP-HPLC on Grace Vydac C18 columns using linear gradients; mobile phase A: 99 % H<sub>2</sub>O/1 % AcCN/0.075 % TFA; mobile phase B: 90 % AcCN/10 % H<sub>2</sub>O/0.1 % (purity > 85 %). Peptides used for IR measurements were lyophilized from 0.05 M aqueous HCl solution (5 ×) to remove the trifluoroacetate counterions.<sup>[20]</sup>

**In situ coupling reaction of peptides:** All in situ coupling reactions on maleimide-functionalized solid-supported membranes were performed in 50 mM PBS pH 6.8 (see the Supporting Information).<sup>[21]</sup>

Received: June 26, 2008

Revised: October 1, 2008

Published online: December 18, 2008

**Keywords:** coiled coils · inhibitors · peptides · solid-supported membranes

[1] D. C. Chan, P. S. Kim, *Cell* **1998**, 93, 681.

[2] D. M. Eckert, P. S. Kim, *Annu. Rev. Biochem.* **2001**, 70, 777.

[3] D. C. Chan, D. Fass, J. M. Berger, P. S. Kim, *Cell* **1997**, 89, 263.

- [4] S. Liu, H. Lu, J. Niu, Y. Xu, S. Wu, S. Jiang, *J. Biol. Chem.* **2005**, *280*, 11259.
- [5] K. Tan, J.-h. Liu, J.-h. Wang, S. Shen, M. Lu, *Proc. Natl. Acad. Sci. USA* **1997**, *94*, 12303.
- [6] C. Cianci, D. R. Langley, D. D. Dischino, Y. Sun, K.-L. Yu, A. Stanley, J. Roach, Z. Li, R. Dalterio, R. Colonna, N. A. Meanwell, M. Krystal, *Proc. Natl. Acad. Sci. USA* **2004**, *101*, 15046.
- [7] R. W. Doms, J. P. Moore, *J. Cell Biol.* **2000**, *151*, 9F.
- [8] J. J. Dwyer, K. L. Wilson, D. K. Davison, S. A. Freel, J. E. Seedorff, S. A. Wring, N. A. Tvermoes, T. J. Matthews, M. L. Greenberg, M. K. Delmedico, *Proc. Natl. Acad. Sci. USA* **2007**, *104*, 12772.
- [9] G. Frey, S. Rits-Volloch, X. Q. Zhang, R. T. Schooley, B. Chen, S. C. Harrison, *Proc. Natl. Acad. Sci. USA* **2006**, *103*, 13938.
- [10] J. M. Kilby, S. Hopkins, T. M. Venetta, B. DiMassimo, G. A. Cloud, J. Y. Lee, L. Alldredge, E. Hunter, D. Lambert, D. Bolognesi, T. Matthews, M. R. Johnson, M. A. Nowak, G. M. Shaw, M. S. Saag, *Nat. Med.* **1998**, *4*, 1302.
- [11] V. N. Malashkevich, D. C. Chan, C. T. Chutkowski, P. S. Kim, *Proc. Natl. Acad. Sci. USA* **1998**, *95*, 9134.
- [12] T. Heimburg, D. Marsh, *Biophys. J.* **1993**, *65*, 2408.
- [13] T. Heimburg, J. Schuenemann, K. Weber, N. Geisler, *Biochemistry* **1996**, *35*, 1375.
- [14] T. Heimburg, J. Schuenemann, K. Weber, N. Geisler, *Biochemistry* **1999**, *38*, 12727.
- [15] A. Muga, H. H. Mantsch, W. K. Surewicz, *Biochemistry* **1991**, *30*, 2629.
- [16] P. B. Harbury, P. S. Kim, T. Alber, *Nature* **1994**, *371*, 80.
- [17] V. D. Trivedi, S.-F. Cheng, C.-W. Wu, R. Karthikeyan, C.-J. Chen, D.-K. Chang, *Protein Eng.* **2003**, *16*, 311.
- [18] S. Faiss, S. Schuy, D. Weisskopf, C. Steinem, A. Janshoff, *J. Phys. Chem. B* **2007**, *111*, 13979.
- [19] M. Schnölzer, P. Alewood, A. Jones, D. Alewood, S. Kent, *Int. J. Pept. Protein Res.* **1992**, *13*, 31.
- [20] V. V. Andrushchenko, H. J. Vogel, E. J. Prenner, *J. Pept. Sci.* **2007**, *13*, 37.
- [21] S. Schuy, B. Treutlein, A. Pietuch, A. Janshoff, *Small* **2008**, *4*, 970–982.
- [22] S. Liu, W. Jing, B. Cheung, H. Lu, J. Sun, X. Yan, J. Niu, J. Farmer, S. Wu, S. Jiang, *J. Biol. Chem.* **2007**, *282*, 9612–9620.